Evidence of X-Shaped Propagation-Invariant Localized Light Waves

Peeter Saari and Kaido Reivelt
Institute of Physics, Riia 142, EE2400 Tartu, Estonia
(Received 27 June 1997)

The peculiar spatiotemporal profile of an optical realization of the nonspreading axisymmetric X wave has been recorded. For treatment of the experiment a simple representation of X-type waves and their correlation with plane waves has been introduced, which covers also a broader class of incoherent wave fields. [S0031-9007(97)04566-3]

PACS numbers: 42.25.Bs, 03.40.Kf, 41.20.Jb, 42.65.Re

Ten years ago Durnin, Miceli, and Eberly [1] reported on the startling first experimental investigation of the so-called nondiffracting Bessel beam, which was formed from a cw laser light by an annular slit and a collimating lens. The beam was found to maintain its sharply peaked radial profile over large distances outclassing the Rayleigh range. During the decade monochromatic Bessel beams have been further extensively studied and applied in both optics and acoustics (see, e.g., Refs. [2–10], and references therein). On the other hand, there have been discovered several classes of nonspreading wideband wave-packet solutions to the linear wave equations of mathematical physics ("focus wave modes," "Bessel-Gauss pulses," "directed energy pulse trains," "electromagnetic bullets," "slingshot pulses," "X waves," etc. [10–18]), which maintain their spatiotemporal localization in the course of propagation in free space. The feasibility of experimental launching has been tested in acoustics for the directed energy pulse train [13] and for the X wave [17]. The acoustical X-type waves are attracting growing interest, particularly, due to the outlook of application in medical ultrasonic imaging [10]. Unfortunately, difficulties with meeting the requirement of ultrawideband spectral content in the case of light field, have obstructed the study of these particlelike solutions in optics. However, recently an optical version of the X wave, named the Bessel-X pulse, was treated theoretically and its propagation-invariant high localization ($\sim 10^{-3}$ mm) as well as an ability to carry arbitrary images diffraction freely over large distances was shown by computer simulations [19,20]. Specially designed femtosecond-duration Bessel-X pulses not only maintain their lateral localization but also the longitudinal one in a dispersive propagation media [21,20]. Such a possibility to suppress the temporal spread caused by the group velocity dispersion has been experimentally verified [22] on subpicosecond laser pulses. To our best knowledge, Ref. [22] gives so far the only experimental test of the feasibility of the optical X waves.

In this Letter we report on experimental measurements of the whole three-dimensional distribution of the field of optical X waves in free space.

In order to make the idea of the experiment better comprehensible, we first discuss different mathematical representations of an X wave as well as its physical nature and generalize the treatment to incoherent fields.

The field of the axisymmetric Bessel beam reads as $U_B(\rho, z, t, k) \propto J_0(\rho k \sin\theta) \times \exp[i(zk\cos\theta - \omega t)]$, where ρ is the transversal distance from the propagation axis z, J_0 is the zeroth-order Bessel function of the first kind, $k = \omega/c$ is the wave number of the monochromatic light, and the parameter θ is referred to as the cone angle or the Axicon angle of the Bessel beam [1,4]. By superimposing Bessel beams with different frequencies and denoting the corresponding Fourier amplitude by $S(k)$, one obtains an integral expression for the X-type field in spectral representation

$$U_X(\rho, z, t) = \int_0^\infty dk\, S(k) U_B(\rho, z, t, k)\,. \qquad (1)$$

With a particular white spectrum $S(k) \propto \exp(-ak)$ exponentially decaying from its maximum at $k = 0$, the integral can be easily taken [16] resulting in a closed analytic expression of the X wave.

By making use of an equality derivable from an integral representation of the Bessel function $J_0(v) = \pi^{-1}\int_0^\pi \cos[v\cos(\phi - \varphi)]\,d\phi$, where φ is an arbitrary angle, we obtain

$$U_X(\rho, z, t) = \frac{1}{\pi}\int_0^\pi d\phi \int_0^\infty dk \times S(k)\cos[\rho k \sin\theta\cos(\phi - \varphi)] e^{iz_t k\cos\theta}, \qquad (2)$$

where substitutions $z_t = z - c't$ and $c' = c/\cos\theta$ define the propagation variable z_t and the speed c' of the pulse's propagation-invariant flight. The integral over k is nothing but an inverse Fourier transform of the cosine-modulated $S(k)$ back to the space-time representation of the pulsed field, which is taken at the point $z_t\cos\theta$. After some manipulation on the trigonometric functions we finally can express the X-wave field via the temporal dependence $A(-ct)$ of the field of the light source:

$$U_X(\rho, z_t) = \int_0^\pi d\phi [A(\mathbf{r}_t\mathbf{n}_/) + A(\mathbf{r}_t\mathbf{n}_\backslash)], \qquad (3)$$

where $\mathbf{r}_t = [\rho\cos\varphi, \rho\sin\varphi, z_t]$ is the radius vector of field point in the copropagating frame

and $\mathbf{n}_{/} = [\sin\theta\cos\phi, \sin\theta\sin\phi, \cos\theta]$, $\mathbf{n}_{\backslash} = [\sin\theta\cos(\phi + \pi), \sin\theta\sin(\phi + \pi), \cos\theta]$ is a pair of unit vectors forming a cone as ϕ runs from 0 to π, which has the top angle 2θ. These unit vectors, as they stand in the scalar-product argument of the field function A, determine directions of pulsed plane wave constituents of the X wave. Hence, according to Eq. (3) the field is built up from interfering pairs of identical bursts of plane waves. Every plane wave pair makes up an X-shaped propagation-invariant interference pattern moving along the axis z with speed $c' = c/\cos\theta$ which is both the phase and the group velocity of the wave field in the direction of the axis z. This speed is superluminal in a similar way as one gets a faster-than-light movement of a bright stripe on a screen when a plane wave light pulse is falling at the angle θ onto the screen plane [23]. The shorter the source pulse, the better the separation and resolution of the branches of the X-shaped profile. In the superposition of all pairs the only point of completely constructive interference is a point of z axis, which becomes the pulse center. In other words, as a result of the integration one gets a field profile reminiscent of the one obtainable by revolving the letter X around its horizontal axis [24]. The highly localized energy "bullet" arises in the center, while the intensity falls off as ρ^{-1} along the branches and much faster in all other directions (see Fig. 1 and Refs. [19,20]). The optical carrier manifests itself as one or more (depending on the pulse length) halo toroids which are nothing but residues of the concentric cylinders of intensity characteristic of the Bessel beam. That is why we use the term "Bessel-X pulse" (or wave) to draw a distinction from carrierless or unipolar pulses.

According to Fig. 1 a straightforward method for recording the field shape would use a CCD camera with a gate in front of it, which should possess a temporal resolution and a variable firing delay both in subfemtosecond range. As such a gate is not realizable, any workable idea of experiment has to resort to a field cross-correlation technique. Fortunately, we can take advantage of the superluminal speed of the Bessel-X pulse, which allows the latter to catch up with a reference plane wave pulse generated in the same optical scheme as depicted in Fig. 2.

A simple geometric consideration shows that the catch-up point, which we further take as the origin of the z axis, is near the rear focal point of the L3 lens (more exactly at the distance $f/\cos\theta$ from the L3 lens, where $f_{\mathrm{L3}} = 56.5$ cm and $\theta = 0.006$ rad in our experiment). If one performs a time-integrated recording of the cross-correlation interference patterns in the radial plane at successive points along the z axis, one gets the spatiotemporal profile of the Bessel-X wave field. Indeed, a 2D photodetector placed in an x-y plane at some distance z records time-integrated intensity distribution given by $\langle U^*U\rangle = \langle U_P^*U_P + U_X^*U_X + 2\,\mathrm{Re}\,U_X^*U_P\rangle$, where the brackets denote the time (or ensemble) averaging, U_P is the plane wave field, the first terms are the intensities of the cross-correlated fields, and the last term corresponds to the interference pattern. By making use of Eq. (3), we obtain

$$\langle U_X^*U_P\rangle = \int_0^{\pi} d\phi[\Gamma_{A,A}(\mathbf{r}_\theta\mathbf{n}_{/}) + \Gamma_{A,A}(\mathbf{r}_\theta\mathbf{n}_{\backslash})], \quad (4)$$

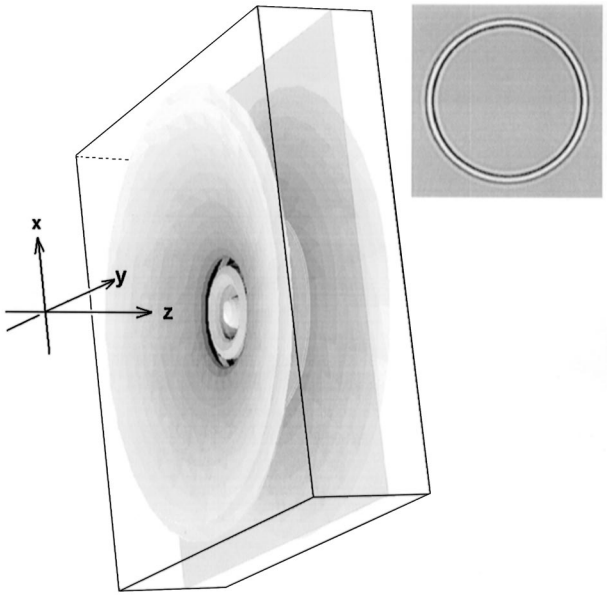

FIG. 1. Intensity profile of a computer-simulated Bessel-X pulse flying in space, shown as surfaces on which the field intensity is equal to a fraction $0.13(\simeq 1/e^2)$ of its maximum value in the central point. The field intensity outside the central bright spot has been multiplied by the radial distance in order to reveal the weak off-axis sidelobes. Inset: Amplitude distribution in the plane shown as intersecting the pulse. The plots have been computed for a 3-fsec near-Gaussian-spectrum source pulse [19,20] with carrier wavelength $\lambda_0 = 0.6$ μm and the angle $\theta = 14°$. For these parameters the dimensions of the plot xyz box are $20 \times 20 \times 6$ μm.

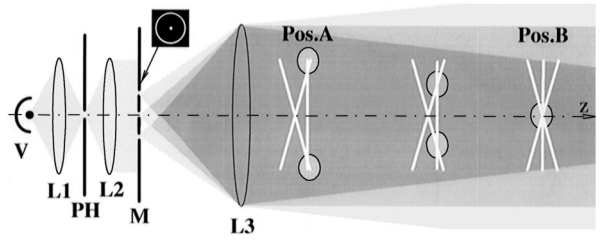

FIG. 2. Optical scheme of the experiment. Mutual instantaneous placement of the Bessel-X pulse and the plane wave pulse is shown for three recording positions (two of which labeled in accordance with Fig. 3). The ovals indicate toroidlike correlation volumes where copropagating Bessel-X and plane wave pulses interfere at different propagation distances along the z axis. L's, lenses; M, mask with Durnin's annular slit and an additional central pinhole for creating the plane wave; PH, cooled pinhole 10 μm in diameter to assure the transversal coherence of the light from the source V. In case source V generates a non-transform-limited pulse or a white cw noise, the bright shapes depict propagation of the correlation functions instead of the pulses.

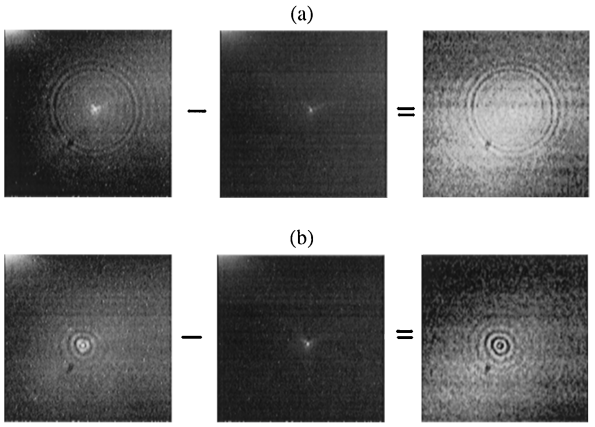

FIG. 3. Samples of the experimental recordings and processing of the intensity distributions measured at the positions along the z axis: (a) at Pos. A and (b) at Pos. B as shown in Fig. 2. Left column, total interference pattern $\langle U^*U\rangle$ of the cross-correlated fields; middle column, lateral intensity distribution $\langle U_X^*U_X\rangle$ of the Bessel-X field alone. In the right column gray (about 50%) corresponds to zero level and dark to negative values. Compare the panels with the inset in Fig. 1.

where the source field autocorrelation function $\Gamma_{A,A}(x) = \langle A^*(s + x)A(s)\rangle_s$ has been introduced. Vectors $\mathbf{n}_/$ and $\mathbf{n}_\backslash$ are the same as in Eq. (3), but in the radius vector $\mathbf{r}_\theta$ the variable $z_t = z - c't$ has been replaced here by $z_\theta = -(1/\cos\theta - 1)z_m$, where z_m is the distance of the recording device from the catch-up point and the very small factor $(1/\cos\theta - 1)$ serves as a "z-axis microscope" which scales the micrometer-range z dependence of the field into a centimeter range. Subtracting from the recorded 3D distribution of the intensity the z-independent ones of the cross-correlating fields, measured with the annular slit or, respectively, the central pinhole in the mask M blocked, one obtains $\langle U^*U\rangle - \langle U_P^*U_P\rangle - \langle U_X^*U_X\rangle \Rightarrow 2\,\mathrm{Re}\langle U_X^*U_P\rangle \equiv I_{X,P}(\rho, z_\theta) = 2\,\mathrm{Re}\int_0^\pi d\phi[\Gamma_{A,A}(\mathbf{r}_\theta\mathbf{n}_/) + \Gamma_{A,A}(\mathbf{r}_\theta\mathbf{n}_\backslash)]$. If we compare this expression with the hypothetically measurable field distribution given as the real part of Eq. (3), we conclude that the experiment reveals the whole spatiotemporal structure of the Bessel-X field. The natural price we have to pay for resorting to the correlation measurements is replacing the function A with its autocorrelation, which is a minor issue in the case of transform-limited source pulses.

Computer simulations (as in Fig. 1) or simple geometrical estimations indicate that if the autocorrelation time of the source field τ exceeds 10 fsec, the X branching occurs too far from the axis z, i.e., in the outer region where the field practically disappears and, with further increase of τ, gradually becomes just a truncated Bessel beam. We took advantage of the insensitivity of Eq. (4) to the source field phase and, in order to achieve a ~3-fsec correlation time in our experiment [25], we used a white light noise from a superhigh pressure Xe-arc lamp instead of a laser as the field source (see Fig. 2). The recordings at 70 points on the z axis (from behind the L3 lens up to a point a few centimeters beyond the origin [26]) with a 0.5-cm step were performed with a cooled CCD camera EDC–1000TE, which has a 2.64 × 2.64 mm working area containing 192 × 165 pixels, and processed by a PC as follows. First, the substraction of the Bessel-X field intensity was performed (see Fig. 3), whereas the same procedure with the plane wave field intensity, due to its practically even distribution, was found to be unnecessary. In order to reduce noise and the dimensionality of the data array, an averaging over the polar angle in every recording was carried out by taking advantage of the axial symmetry of the field. Thus we got a 1D array containing up to a hundred significant elements from every 192 × 165 matrix recorded. Seventy such arrays formed a matrix, which, having in mind the known symmetry of the real part of Eq. (4), was mirrored in the lateral and the axial planes. The result is compared in Fig. 4 with the Bessel-X field distribution in an axial plane, computed from Eq. (1) for a model spectrum. The latter was taken as a convex curve covering the whole visible region from blue to near infrared (up to 0.9 μm) in order to simulate the effective light spectrum in the experiment, which is a product of the Xe-arc spectrum and the sensitivity curve of the camera. The central (carrier) frequency was chosen corresponding to wavelength 0.6 μm which had been determined from the fringe spacing of an autocorrelation pattern recorded for the light source with the same CCD camera. The left- and right-hand tails of the central X-like structure are more conspicuous in the experimental pattern due to unevenness of the real Xe-arc spectrum. The different scaling of the horizontal axes of the two panels is in accordance with the z axis "magnification" factor of the experimental setup.

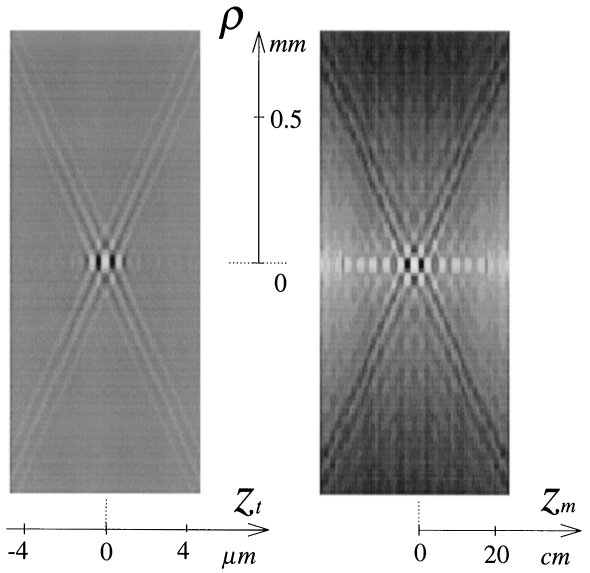

FIG. 4. Comparison of the result of the experiment (right panel) with a computer-simulated Bessel-X pulse field (left panel).

Observing the obvious agreement between theoretical and experimental patterns, we arrive at a conclusion that we have really recorded the characteristic spatiotemporal profile of an optical realization of the nonspreading axisymmetric X wave. As a matter of fact, we have experimentally studied a light field with localized propagation-invariant mutual coherence function and its X-shaped profile as well as have generalized the theoretical treatment of nonspreading pulses to the broader class of incoherent fields [27]. We hope that broadband stochastic wave fields with nonspreading coherence introduced here will deserve no less attention than localized solutions to deterministic wave equations have received so far.

This research was supported by Estonian Science Foundation Grant No. 2267 and, in its initial stage, by Grant No. LL8100 from the Joint Fund Program of Estonia with the International Science Foundation.

[1] J. Durnin, J. J. Miceli, Jr., and J. H. Eberly, Phys. Rev. Lett. **58**, 1499 (1987).
[2] T. Wulle and S. Herminghaus, Phys. Rev. Lett. **70**, 1401 (1993).
[3] A. Vasara, J. Turunen, and A. T. Friberg, J. Opt. Soc. Am. A **6**, 1748 (1989).
[4] R. M. Herman and T. A. Wiggins, J. Opt. Soc. Am. A **8**, 932 (1991).
[5] S. Ruschin, J. Opt. Soc. Am. A **11**, 3224 (1994).
[6] Z. Bouchal, J. Mod. Opt. **40**, 1325 (1993).
[7] V. P. Koronkevich, I. A. Mikhaltsova, E. G. Churin, and Yu. I. Yurlov, Appl. Opt. **34**, 5761 (1995).
[8] F. Gori, G. Guattari, and C. Padovani, Opt. Commun. **64**, 491 (1987).
[9] S. Chávez-Cerda, G. S. McDonald, and G. H. C. New, Opt. Commun. **123**, 225 (1996).
[10] J. Lu, IEEE Trans. Ultrason. Ferroelectr. Freq. Control **42**, 1050 (1995).
[11] J. N. Brittingham, J. Appl. Phys. **54**, 1179 (1983).
[12] R. W. Ziolkowski, Phys. Rev. A **39**, 2005 (1989).
[13] R. W. Ziolkowski, D. K. Lewis, and B. D. Cook, Phys. Rev. Lett. **62**, 147 (1989).
[14] R. W. Ziolkowski, I. M. Besieris, and A. M. Shaarawi, J. Opt. Soc. Am. A **10**, 75 (1993).
[15] P. L. Overfelt, Phys. Rev. A **44**, 3941 (1991).
[16] J. Lu and J. F. Greenleaf, IEEE Trans. Ultrason. Ferroelectr. Freq. Control **39**, 19 (1992).
[17] J. Lu and J. F. Greenleaf, IEEE Trans. Ultrason. Ferroelectr. Freq. Control **39**, 441 (1992).
[18] J. Fagerholm, A. T. Friberg, J. Huttunen, D. P. Morgan, and M. M. Salomaa, Phys. Rev. E **54**, 4347 (1996).
[19] P. Saari, in *Ultrafast Processes in Spectroscopy*, edited by O. Svelto, S. De Silvestri, and G. Denardo (Plenum, New York, 1996), p. 151.
[20] P. Saari and H. Sõnajalg, Laser Phys. **7**, 32 (1997).
[21] H. Sõnajalg and P. Saari, Opt. Lett. **21**, 1162 (1996).
[22] H. Sõnajalg, M. Rätsep, and P. Saari, Opt. Lett. **22**, 310 (1997).
[23] That is why there is nothing unphysical with the superluminal movement of the X wave: like the light stripe on the screen it also cannot carry any causal signal between two points along the axis. See Refs. [1,4,12,14,16] for a thorough discussion of this issue and other typical curiosities of the propagation-invariant solutions, not all of which are inherent in physically launchable finite-aperture (and consequently, finite-propagation-length) realizations considered here.
[24] Equation (3) is preferred over Eq. (1) also from the point of view of computer simulations, since the latter representation as a polychromatic superposition of Bessel beams contains an integrand less suited to numerical intergration, whereas an analytical closed form for the integral of Eq. (1), if optically realizable spectra $S(k = 0) = 0$ are considered, has been found only for a near-Gaussian source pulse [19,20].
[25] K. Reivelt and P. Saari, in *Technical Digest of X International Symposium "Ultrafast Phenomena in Spectroscopy"* (Institute of Physics, University of Tartu, Tartu, Estonia, 1997), p. 126.
[26] A few recordings beyond the origin proved already the known mirror symmetry of the field and therefore we did not carry out any full-length measurement series there. Also we did not study the region around and beyond the maximum propagation depth $\sim D/2\tan\theta$ of Bessel-X waves or their Bessel-beam constituents with limited aperture of diameter D [1]. In this region a few meters away from the L3 lens, aside from difficulties of signal recording, the field looses its interesting features and decays into a diverging beam of an expanding-ring-like lateral profile. The details of the decay, as it follows from various numerical simulations in the literature on monochromatic Bessel beams, depend upon concrete aperture function.
[27] A generalization of Bessel beams to monochromatic spatially incoherent propagation-invariant beams has been accomplished by A. T. Friberg, A. Vasara, and J. Turunen, Phys. Rev. A **43**, 7079 (1991).